Synthesis and Properties of Zn−Al Layered Double Hydroxides Containing Ferrocenecarboxylate Anions

Sandra Gago,[a] Martyn Pillinger,*[a] Teresa M. Santos,[a] João Rocha,[a] and Isabel S. Gonçalves*[a]

Keywords: Hydroxides / Layered compounds / Ferrocene / Host-guest systems / Organic-inorganic hybrid composites

Zn–Al layered double hydroxides (LDHs) intercalated by ferrocenecarboxylate (FcCOO) and 1,1′-ferrocenedicarboxylate [$Fc(COO)_2$] anions have been prepared by co-precipitation from aqueous solution. The Zn/Al ratio in the final materials was in the range of 1.8–1.9. Powder X-ray diffraction (XRD) indicates that the material Zn_2Al–$Fc(COO)_2$ contains a monolayer of guest anions resulting in a basal spacing of 15.5 Å. The material Zn_2Al–FcCOO exhibits a basal spacing of 20.0 Å, consistent with the formation of a bilayer of organometallic guest species. FTIR, FT Raman and ^{13}C MAS NMR spectroscopy confirm the presence of structurally intact ferrocenecarboxylate and 1,1′-ferrocenedicarboxylate anions. The nature of the Al centers in the samples was probed by 1- and 2-D (triple-quantum) ^{27}Al MAS NMR spectroscopy. Thermal properties were studied by thermogravimetric analysis and by measuring powder XRD patterns at increasing temperatures in the range of 25–450 °C. Up to 160 °C the materials lose interlayer water molecules. Dehydration of Zn_2Al–$Fc(COO)_2$ prompts reorientation of the ferrocene guest anions, resulting in the formation of a collapsed phase with an interlayer separation of 12.3 Å. The structural transformation is fully reversible upon hydration. Heat treatment of Zn_2Al–FcCOO only resulted in a gradual contraction of the interlayer separation and not the formation of a collapsed phase.

Introduction

Layered double hydroxides (LDHs), also known as anionic clays or hydrotalcite-like compounds, are an important class of ionic lamellar solids.[1] The structures of LDHs consist of positively charged mixed metal hydroxide layers separated by charge-balancing anions and water molecules. A broad range of compositions of the type $[M^{2+}_{1-x}M^{3+}_{x}(OH)_2](A^{m-})_{x/m}\cdot nH_2O$ (M^{2+} = Mg^{2+}, Zn^{2+}, Ni^{2+} etc., M^{3+} = Al^{3+}, Cr^{3+}, Ga^{3+} etc.) are possible, in which the M^{2+} and M^{3+} metal ions occupy octahedral positions in the hydroxide layers. The gallery anions A^{m-} are exchangeable, giving rise to a rich intercalation chemistry,[2] and the guest species may be organic or inorganic, simple or complex.[3] LDHs find uses as catalysts and catalyst supports,[4] adsorbents, anion scavengers, anion exchangers, polymer stabilizers, and antacids.[1] The synthesis of LDHs intercalated by metal coordination compounds and oxometalates was reviewed recently.[3b] Apart from cyano complexes, e.g. $Fe(CN)_6^{3-}$ and $Fe(CN)_6^{4-}$, there are few examples of LDHs intercalated by organometallic anions, especially those containing cyclopentadienyl (Cp = η^5-C_5H_5) and η^6-arene groups. Two exceptions are LDH intercalates containing ferrocenesulfonate[5] and ferrocenebutyrate anions,[6] and their use in clay-modified electrodes. These hybrid materials may also exhibit interesting photochemical or photophysical properties.[7] In the present work, Zn−Al LDHs intercalated by ferrocenecarboxylate and 1,1′-ferrocenedicarboxylate anions have been synthesized directly by co-precipitation from aqueous solution. The materials were characterized by powder X-ray diffraction, FTIR and Raman spectroscopy, magic-angle-spinning NMR (^{13}C, ^{27}Al) spectroscopy, and thermogravimetric analyses (TGA). As will be described, the interlayer arrangement of organometallic anions depends on a number of factors, including the presence of one or two carboxylate substituents in the guest molecules and the degree of hydration of the LDH. Such factors have previously been shown to be important for LDHs intercalated by organic carboxylic acids.[8,9] In this paper comparison will be made with these studies, in particular those concerning the aromatic guests terephthalate and benzoate.

Results and Discussion

Structural and Compositional Analysis

The structural formulae of the synthesized samples $Zn_2Al-Fc(COO)_2$ and $Zn_2Al-FcCOO$ conform to the de-

[a] Department of Chemistry, CICECO, University of Aveiro, 3810-193 Aveiro, Portugal
Fax: (internat.) +351-234-370084
E-mail: igoncalves@dq.ua.pt

Table 1. Chemical compositions and diffraction data for the LDH intercalates

Composition	x[a]	d(003) [Å]	c[b] [Å]	a (Å)	A_c[c] [Å^2/e]	t[d] [Å]
$Zn_{3.8}Al_2(OH)_{11.6}[Fc(COO)_2]\cdot 7H_2O$	0.345	15.5	46.35	3.04	23.2	115
$Zn_{3.5}Al_2(OH)_{11}[FcCOO]_2\cdot 8H_2O$	0.364	20.0	60.05	3.04	22.0	233

[a] Molar ratio $x = Al^{3+}/(Zn^{2+} + Al^{3+})$. [b] Lattice parameters a and c calculated from d(110) and d(003) planes, respectively. [c] Area per unit charge in the brucite-like layer, $A_c = (a^2\sin 60)/x$. [d] Average crystallite sizes calculated from the (003), (006), (009), (0012) and (0015) planes employing the Debye−Scherrer equation.

sired stoichiometric compositions except that the final Zn/Al atomic ratios are slightly lower than the value of 2.0 used in the starting solution (Table 1). This indicates an incomplete precipitation of the divalent cation, possibly due to the fact that the final pH used in the syntheses (7−8) is at the low end of the range appropriate for the synthesis of Zn−Al LDHs (7−9).[1]

The powder XRD patterns of $Zn_2Al-Fc(COO)_2$ and $Zn_2Al-FcCOO$, recorded at ambient temperature in the range of 3−70 °2θ, are typical of reasonably well-crystallized hydrotalcite-type compounds (Figure 1). Indexing was based on rhombohedral symmetry (polytype $3R_1$). The (00l) basal reflections can be easily identified as a series of symmetric, equally spaced peaks at angles below 30 °2θ. The high intensities combined with broad line-shapes indicate that the materials are of relatively high crystallinity but form as small crystallites. Furthermore, the alternation of the intensities of successive 00l reflections is indicative of a high concentration of electron density in the midplane of the interlayer region.[8a] The average crystallite sizes in the z direction were estimated from the (003), (006), (009), (0012) and (0015) planes using Scherrer's equation $L = 0.9\lambda/\beta_c\cos\theta$, where L is the crystallite size in Å along a line normal to the reflecting plane, λ is the wavelength of the radiation used, β_c is the instrument-corrected width of a reflection at half-height expressed in radians of 2θ, and θ is the Bragg diffraction angle. Values of 115 and 233 Å were found for $Zn_2Al-Fc(COO)_2$ and $Zn_2Al-FcCOO$, respectively (Table 1). The powder XRD patterns of the two LDHs also contain broad, asymmetric (*hkl*) reflections above ca. 2θ ≥ 30°, characteristic of turbostratic layered structures. Many organic-anion-pillared LDHs exhibit similar structural features.[10] The turbostratic effect is caused by a decrease in the ordering along the stacking axis due to the loss of van der Waals interactions between adjacent layers and the absence of a densely packed interlayer space formed by high charge density anions such as carbonate. On comparing the powder XRD patterns shown in Figure 1, it is evident that $Zn_2Al-FcCOO$ exhibits increased turbostratic disorder because the *hkl* reflections are broader and less intense, and in fact several are not observed. These differences are understandable when we consider the two types of guest species and the corresponding interlayer arrangements (see below).

The lattice parameter a, which corresponds to the average metal-metal distance in the layers, was calculated to be 3.04 Å for both samples ($a = 2d_{110}$). The parameter c was calculated as three times the spacing of the diffraction maximum

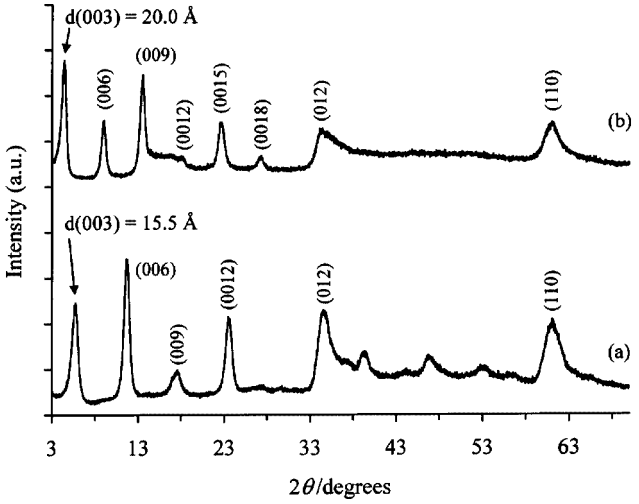

Figure 1. Powder XRD patterns at room temperature of (a) $Zn_2Al-Fc(COO)_2$ and (b) $Zn_2Al-FcCOO$

corresponding to planes (003), leading to values of 46.35 Å for $Zn_2Al-Fc(COO)_2$ and 60.05 Å for $Zn_2Al-FcCOO$. If the thickness of the brucite-like layer is taken as 4.77 Å, the gallery heights are 10.7 Å and 15.2 Å, respectively. In this work, the dimensions of the guest molecules have been estimated by using the structures of the heterobimetallic compounds $[LaL^1_3(CH_3OH)_4]_\infty$ (L^1 = 1,1′-ferrocenedicarboxylate) and $La_2L^2_6(CH_3OH)_2(H_2O)_5$ (L^2 = ferrocenecarboxylate), reported by Qing-jin and co-workers.[11] In $[LaL^1_3(CH_3OH)_4]_\infty$, two types of ferrocenedicarboxylato(2−) ligands exist, differing in their conformations. One of these is antiperiplanar with a torsion angle of 180°. The longest dimension of this molecule corresponds to one of the O···O distances and is equal to 7.48 Å. Taking into account the van der Waals radius of oxygen, this distance becomes 10.52 Å which is very similar to the observed gallery height. It is therefore reasonable to assume that the interlayer of $Zn_2Al-Fc(COO)_2$ consists of a monolayer of guest species with the longest dimension of each anion perpendicular to the brucite-like layers, as depicted in Figure 2. In this orientation, the area occupied by each molecule in the xy plane is equal to about 40 Å^2. The area per unit charge of the host lattice is given by $A_c = (a^2\sin 60)/x$, where a is the lattice parameter and x is the molar ratio of trivalent to total cations. For $Zn_2Al-Fc(COO)_2$, a = 3.04 Å and x = 0.345, and so A_c = 23.2 Å^2 (Table 1). Hence, the area available per divalent anion is approximately 46.4 Å^2. It follows that in a monolayer of 1,1′-ferrocenedicarboxyl-

ate anions, the host layer charge can be balanced although relatively close packing of guest molecules is required.

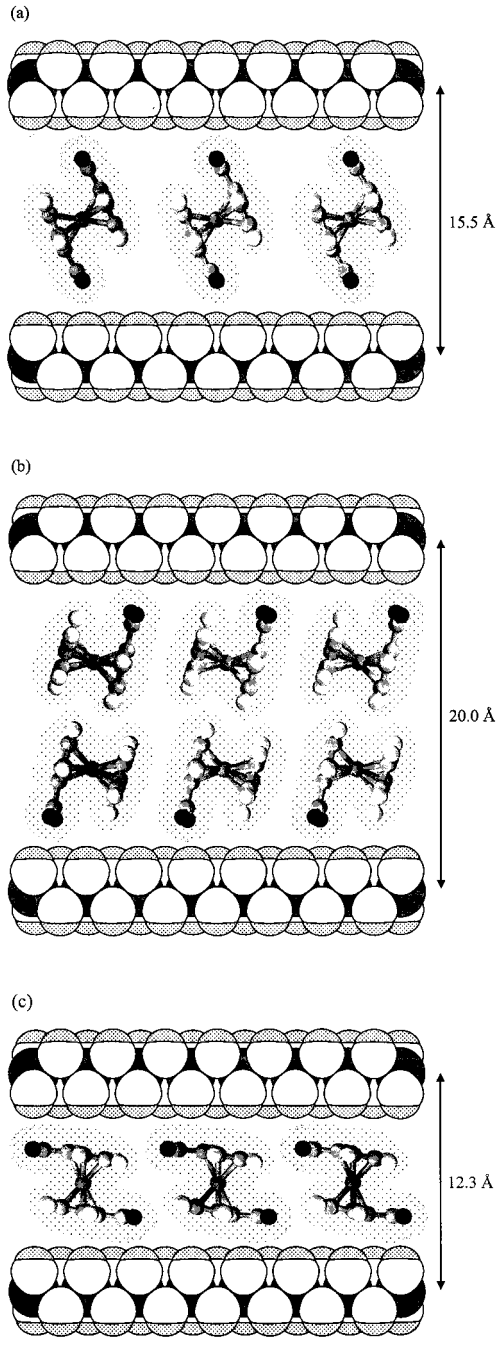

Figure 2. Models for the interlayer arrangement of guest species in (a) $Zn_2Al-Fc(COO)_2$ (fully hydrated sample = expanded phase), (b) $Zn_2Al-FcCOO$ (fully hydrated sample) and (c) $Zn_2Al-Fc(COO)_2$ (dehydrated sample = collapsed phase)

It is clear from the above calculations that the ferrocenecarboxylate anion would not be capable of spatially balancing the host layer charge of a Zn_2Al LDH, if arranged in a monolayer. The observed gallery height of $Zn_2Al-FcCOO$ is 15.2 Å, which suggests that a bilayer-like structure exists within the gallery. Figure 2(b) shows a possible arrangement of guest anions for which the calculated basal spacing exactly matches the observed value. Morlat-Thérias et al. reported Zn−Cr LDHs pillared by ferrocene mono- and disulfonate anions.[6] The basal spacings observed for their materials (20.0 and 15.0 Å, respectively) are very similar to those found in the present work for the corresponding carboxylate derivatives. It is worth noting that the interlayer arrangements for LDHs intercalated by mono- and disubstituted ferrocenes are similar to those usually reported for LDHs pillared by benzoate and terephthalate anions, respectively (with $M^{2+}/M^{3+} \approx 2$). Like 1,1′-ferrocenedicarboxylate, terephthalate anions tend to adopt a vertical orientation within the interlayer, at least under fully hydrated conditions.[3a,8,12] Benzoate anions form bilayer-like structures[8b] or monofilms of interdigitated species as found for methyl orange.[13] In all these LDH intercalates, the preferred orientation of the guest species permits a maximum interaction with the layers through hydrogen bonding with the layer hydroxyl groups, and at the same time the hydrophobic aromatic groups are located within the center of the galleries, as far apart as possible from the hydrophilic layer hydroxyls.

The organometallic-LDHs were further characterized by FTIR, Raman and MAS NMR spectroscopy. In the high frequency region (4000−2000 cm^{-1}), the IR spectra are dominated by broad bands at about 3410 cm^{-1}, attributable to the O−H stretches of weakly hydrogen-bonded water molecules and layer hydroxyl groups. A weak shoulder at about 3090 cm^{-1} (only observed for $Zn_2Al-FcCOO$) can be assigned to the C−H stretch of the cyclopentadienyl (Cp) rings of the guest. This band is stronger in the Raman spectra, and is located at 3108 cm^{-1} for $Zn_2Al-FcCOO$ and 3117 cm^{-1} for $Zn_2Al-Fc(COO)_2$. In the IR spectra, the C−C stretching vibration for the Cp rings appears at 1472 cm^{-1} for $Zn_2Al-FcCOO$ and 1487 cm^{-1} for $Zn_2Al-Fc(COO)_2$, weakly shifted compared with the corresponding bands for ferrocenecarboxylic acid (1475 cm^{-1}) and 1,1′-ferrocenedicarboxylic acid (1492 cm^{-1}). The two acids display strong bands in the solid state at about 1665 and 1300 cm^{-1}, due to C=O and C−O stretches. These bands are not observed in the spectra of the LDH intercalates, indicating that the guest species are deprotonated. This is confirmed by the presence of strong peaks at 1525 and 1391 cm^{-1} for $Zn_2Al-FcCOO$, and 1554 and 1401 cm^{-1} for $Zn_2Al-Fc(COO)_2$, assigned to $\nu_{as}(OCO)$ and $\nu_s(OCO)$, respectively. Below 750 cm^{-1}, the IR spectra of the two LDHs contain some bands due to the guest species (515 and 485 cm^{-1}) in addition to peaks arising from the host lattice. A broad band at about 630 cm^{-1} is due either to a vibrational mode of the hydroxyl groups and water or to a metal−oxygen vibration $\nu(M-O)$.[14] Two peaks at about 560 and 427 cm^{-1} can be attributed to $\nu(M-O)$ and $\delta(M-O-M)$, respectively. In the Raman spectra, the low frequency region is dominated by the intense ν_1 skeletal frequency at 324 cm^{-1} for $Zn_2Al-Fc(COO)_2$ and 314 cm^{-1} for $Zn_2Al-FcCOO$, both of which are weakly shifted compared with the corresponding bands for $Fc(COOH)_2$ and FcCOOH.

Figure 3 shows the ^{13}C CP MAS NMR spectra of $Fc(COOH)_2$, FcCOOH and the corresponding organometallic-LDHs. Ferrocenecarboxylic acid gives rise to peaks at δ = 180.7 ppm due to the carboxyl carbon and δ = 70.8 ppm (with shoulders) due to the Cp carbons. A resolved shoulder at δ = 72.7 ppm can be attributed to the Cp carbon atom that is attached to the carboxylic acid group (*ipso* carbon). Similarly, 1,1′-ferrocenedicarboxylic acid gives rise to peaks at δ = 175.1 and 73.2 ppm, although in this case no resolved shoulder was observed for the *ipso* carbon. The main difference between these spectra and those of the organometallic-LDHs is that the peaks due to the *ipso* carbon atoms are shifted considerably to lower field, presumably due to deprotonation of the carboxylic acid groups. The ^{27}Al MAS NMR spectrum of $Zn_2Al-Fc(COO)_2$ contains a sharp peak at δ = 14 ppm with a broad low-frequency shoulder, assigned to octahedral aluminium (see a in Figure 4). Similar spectra have been reported in the literature for $Zn-Al-CO_3$ and $Mg-Al-CO_3$ LDHs.[15,16] The sheared triple-quantum ^{27}Al MAS NMR spectrum of this sample clearly shows the existence of two distinct Al sites (overlapping resonances S1 and S2, see b in Figure 4). The peak S1, at δ ca. 16 (F1) [δ ca. 14 (F2)], displays a distribution of isotropic chemical shifts. We speculate that this may be due to the presence of a range of slightly different local Al environments generated by the random insertion of Al in the layers.[16] The low-frequency F2 shoulder (S2) is essentially undistributed but it has an average quadrupole coupling constant larger than S1. Similar 1-D and 2-D spectra were obtained for $Zn_2Al-FcCOO$ (not shown).

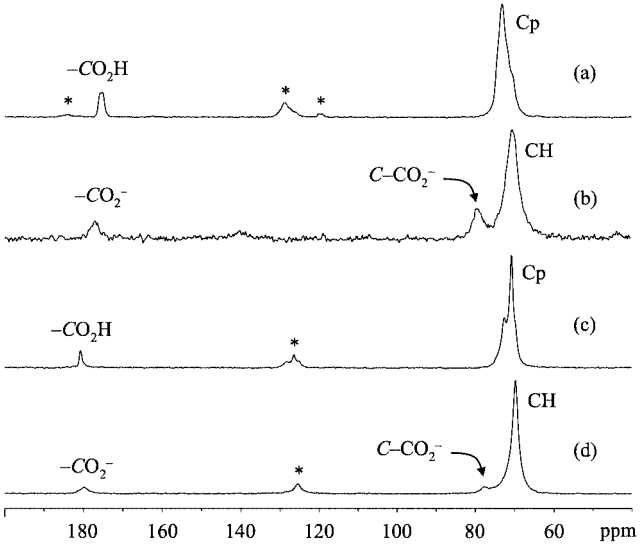

Figure 3. ^{13}C CP MAS NMR spectra of (a) $Fc(COOH)_2$, (b) $Zn_2Al-Fc(COO)_2$, (c) FcCOOH and (d) $Zn_2Al-FcCOO$; spinning side-bands are indicated with an asterisk

Thermal Properties

The TGA traces for $Zn_2Al-Fc(COO)_2$ and $Zn_2Al-FcCOO$ indicate three general regions of mass loss

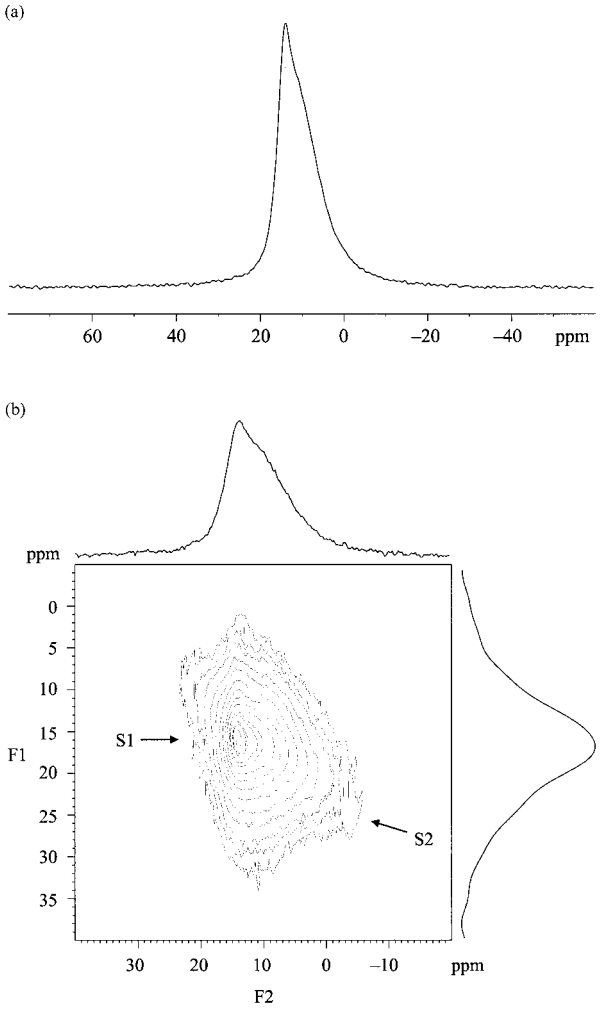

Figure 4. (a) ^{27}Al MAS NMR spectrum of $Zn_2Al-Fc(COO)_2$ and (b) sheared 3Q ^{27}Al MAS NMR spectrum of $Zn_2Al-Fc(COO)_2$

(Figure 5), the first two of which overlap to some extent. The first step, corresponding to removal of interlayer water, extends from room temperature to approximately 180 °C for $Zn_2Al-Fc(COO)_2$ (13.1% mass loss, DTG_{max} = 140 °C) and 160 °C for $Zn_2Al-FcCOO$ (10.6% mass loss, DTG_{max} = 80 °C). The second step, which takes place in the 180–240 °C range for $Zn_2Al-Fc(COO)_2$ (DTG_{max} = 214 °C) and 160–230 °C for $Zn_2Al-FcCOO$ (DTG_{max} = 196 °C), can be assigned to partial dehydroxylation of the double hydroxide layers.[17] The third step extends from about 280 °C to 520 °C and can be attributed to complete dehydroxylation and partial elimination/decomposition of the organometallic anions. The mass loss in this range is higher for $Zn_2Al-FcCOO$ (28.1%) than for $Zn_2Al-Fc(COO)_2$ (20.2%), consistent with the fact that the former has approximately double the number of intercalated ferrocenyl units due to the lower anion charge.

Powder XRD diagrams of $Zn_2Al-Fc(COO)_2$, recorded at increasing temperatures in the range of 25–450 °C, are shown in Figure 6. Only the basal reflections are displayed from which the interlayer spacing of the LDH may be deduced. As described above, the synthesized

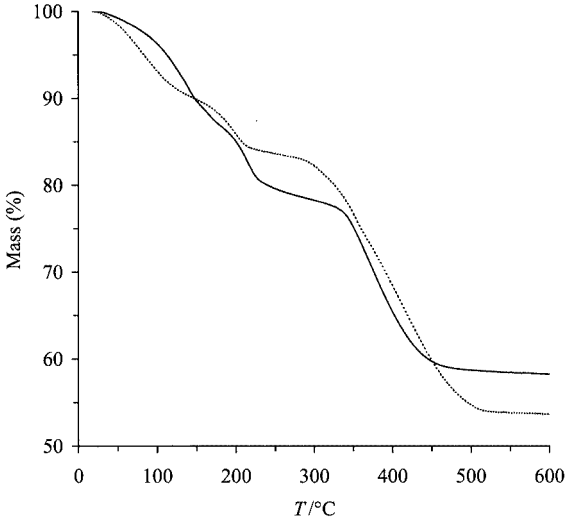

Figure 5. TGA curves for $Zn_2Al-Fc(COO)_2$ (——) and $Zn_2Al-FcCOO$ (− − −)

$Zn_2Al-Fc(COO)_2$ consists of a single expanded phase at room temperature characterized by a basal spacing of 15.5 Å. At 120 °C, the expanded phase can still be identified, although the basal reflections are reduced in intensity and shifted slightly to higher angles. In addition to this phase, a new "collapsed phase" is present characterized by a basal spacing of 12.3 Å. At this temperature, the water content was estimated to be 59% of the initial total. Further heating to 160 °C resulted in complete transformation of the expanded phase to the collapsed phase (water content = 19% of initial total). The basal spacing of 12.3 Å suggests a gallery height of 7.5 Å which fits very well with a model where the shortest dimension of the guest molecules is nearly perpendicular to the host layers (see c in Figure 2). We therefore conclude that removal of interlayer water is accompanied by a reorientation of the organometallic anions.[18] It can be assumed that the ferrocenyl units do not lie completely flat but are tilted slightly with respect to the host layers in order to maintain a hydrogen-bonding interaction between the carboxyl groups and hydroxide layers. The (003) reflection of the collapsed phase did not change much up to 300 °C, despite partial dehydroxylation of the layers. Transformation to an amorphous phase occurred above this temperature, i.e. during the third stage of weight loss observed by TGA. In a separate experiment, a sample of $Zn_2Al-Fc(COO)_2$ was heated to 160 °C and, after measuring the powder XRD pattern at this temperature, cooled to room temperature over ca. 15 min (under moist air), and the powder XRD pattern measured again (Figure 7). The results show complete recovery of the expanded phase, indicating that the structural transformation is fully reversible upon hydration. A TGA of the sample after measuring the powder XRD indicated that the total water content was equal to the initial value, within experimental error. The recovery of the expanded phase demonstrates that heat treatment (up to 160 °C) does not result in covalent grafting of the anions to the hydroxyl layers. These results are similar to those reported by Kooli et al. for a Mg_2Al-TA LDH (TA = terephthalate) prepared by co-precipitation at constant pH.[8b] Thus, it was found that the terephthalate anion initially adopts a vertical orientation between the layers, but above 150 °C the expanded structure collapses, with a shift in the position of the (003) reflection from 14.6 to 8.9 Å suggesting a horizontal arrangement for the anion. Cooling of the sample to room temperature under moist air led to complete recovery of the vertical arrangement.

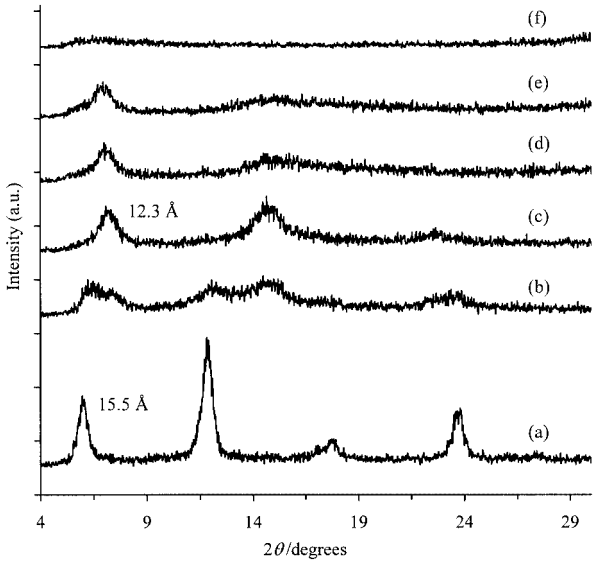

Figure 6. Powder XRD patterns of $Zn_2Al-Fc(COO)_2$ recorded at (a) room temperature, (b) 120 °C, (c) 160 °C, (d) 230 °C, (e) 300 °C and (f) 450 °C; the *d*(003) spacings for the expanded (15.5 Å) and collapsed (12.3 Å) phases are indicated

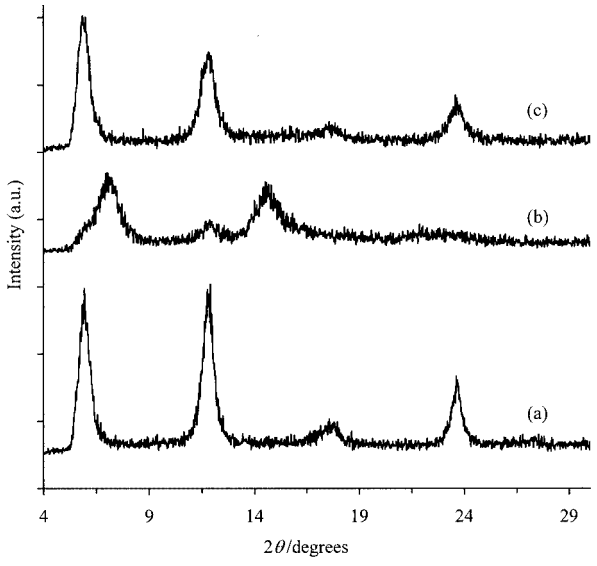

Figure 7. Powder XRD patterns of $Zn_2Al-Fc(COO)_2$ recorded at (a) room temperature, (b) 160 °C and (c) room temperature (after cooling the sample from 160 °C under moist air)

Powder XRD diagrams of $Zn_2Al-FcCOO$, recorded at increasing temperatures in the range of 25−450 °C, did not indicate the formation of a new collapsed phase (Figure 8). Instead, there was a gradual contraction of the interlayer separation up to 160 °C, as evidenced by a slight shift of the basal reflections to higher 2θ values [the (003) peak was not clearly observed in these diffraction patterns, probably due to the nature of the sample holder]. At 230 °C, the (00*l*) reflections had disappeared and only a very broad weak feature was observed between 13 and 20 °2θ. The layered structure was therefore severely disrupted by the partial dehydroxylation which, as revealed by the TGA results, took place in the range 160−230 °C. Transformation to an amorphous phase was complete at 300 °C and no further change took place up to 450 °C.

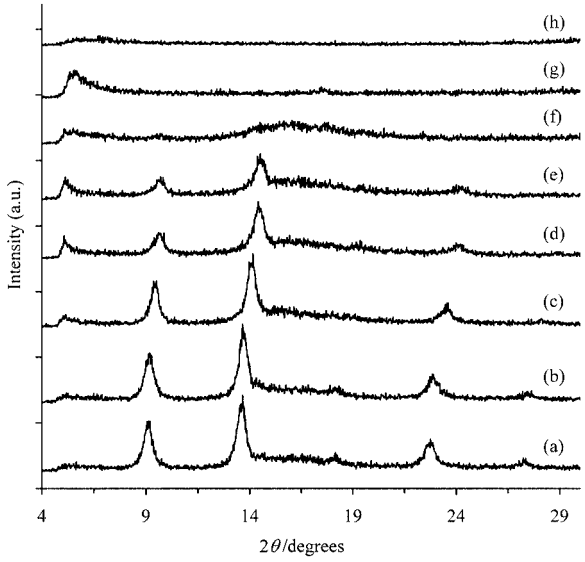

Figure 8. Powder XRD patterns of $Zn_2Al-FcCOO$ recorded at (a) room temperature, (b) 50 °C, (c) 80 °C, (d) 120 °C, (e) 160 °C, (f) 230 °C, (g) 300 °C and (h) 450 °C

Concluding Remarks

Zn−Al layered double hydroxides intercalated by ferrocene guests anions have successfully been prepared by co-precipitation from aqueous solution. In the case of 1,1-ferrocenedicarboxylate, the interlayer separation for the fully hydrated material indicates that the guest species adopt an antiperiplanar conformation and are arranged in a monolayer with the longest dimension perpendicular to the host layers. As observed for many organic-anion-pillared LDHs, water plays a critical role in stabilizing the expanded structure. Heat treatment results in a reorientation of the guest species such that the shortest dimension is nearly perpendicular to the host layers. The resultant collapsed phase is quite stable − the layered structure can still be identified by powder XRD after heat treatment at 300 °C. In the case of ferrocenecarboxylate guest anions, we conclude that bilayer structures are formed in the interlayer. The carboxyl groups are probably linked by hydrogen bonding to the hydroxide sheets with the aromatic groups located within the center of the gallery. Such an arrangement would result in a hydrophobic membrane-like region. This material may therefore have interesting adsorption properties, e.g. the ability to take up organic molecules (and swell in a direction perpendicular to the layers). The interlayer region may also provide a novel environment for photochemical reactions of photoactive molecules. These studies are currently under way in our laboratories in addition to efforts to prepare LDHs containing other types of organometallic anions.

Experimental Section

Materials and Methods: The reagents $Zn(NO_3)_2{\cdot}6H_2O$ (Riedel-de Haën), $Al(NO_3)_3{\cdot}9H_2O$ (Riedel-de Haën), 50% aqueous NaOH (Aldrich), 1,1′-ferrocenedicarboxylic acid [$Fc(COOH)_2$, Fluka] and ferrocenecarboxylic acid (FcCOOH, Fluka) were obtained from commercial sources and used as received.

Microanalyses for CHN were carried out at the Instituto de Tecnologia Química e Biológica, Oeiras, Portugal. Zn, Al and Fe were determined by ICP-OES at the Central Laboratory for Analysis, University of Aveiro (E. Soares). Room temperature powder XRD data were collected on a Philips X'pert diffractometer with a curved graphite monochromator (Cu-K_α radiation) in a Bragg−Brentano para-focusing optics configuration. Samples were step-scanned in 0.02 °2θ steps with a counting time of 1 s per step. The XRD measurements as a function of temperature were carried out in situ using the same diffractometer equipped with an Anton-Parr GmbH HTK16 high temperature chamber containing a Pt heating filament and a Pt−Pt/Rh (10%) thermocouple. The powdered sample was deposited on the filament which also acts as the sample holder. Heating rates of 10 °C min^{-1} were used. At a given temperature, samples were step-scanned in 0.02 °2θ steps with a counting time of 0.6 s per step. TGA studies were performed using a Shimadzu TGA-50 system at a heating rate of 5 °C min^{-1} under nitrogen.

IR spectra were obtained with KBr pellets using an FTIR Mattson-7000 infrared spectrophotometer. Raman spectra were recorded on a Bruker RFS100/S FT instrument (Nd:YAG laser, 1064 nm excitation, InGaAs detector). Solid-state NMR spectra were measured at 100.62 MHz for ^{13}C and 104.26 MHz for ^{27}Al with a (9.4 T) wide bore Bruker Avance 400 spectrometer. ^{13}C CP MAS NMR spectra were acquired with a 4 μs 90° proton pulse and 2 ms contact time with spinning rates of 7−8.5 kHz and 4 s recycle delays. Chemical shifts are quoted in ppm relative to TMS. Single-quantum ('conventional') ^{27}Al MAS NMR spectra were acquired using short and powerful radio-frequency pulses (0.6 μs, corresponding to π/12 pulses), a spinning rate of 14 kHz and a recycle delay of 1 s. Chemical shifts are quoted in ppm relative to $Al(H_2O)_6^{3+}$. The two-dimensional triple-quantum (3Q) ^{27}Al MAS NMR spectra were acquired using the three pulse z-filter sequence.[19,20] The lengths of the two hard pulses were 2.4 μs and 0.7 μs (radio-frequency magnetic field amplitude ν_1 = 150 kHz), and the length of the soft pulse was 11 μs (ν_1 = 7.5 kHz). The MAS rate was 14 kHz. 114 data points were acquired in the t_1 domain in increments of $(1/2\nu r)$ = 35.71 μs. The ppm scale of the sheared spectra was referenced to ν_0 frequency in the ν_2 domain and to $1.42\nu_0$ in the ν_1 domain (high-resolution dimension after shearing). The reference was $Al(H_2O)_6^{3+}$.

Sample Preparation: The LDHs were prepared by a co-precipitation method similar to that described by Drezdon.[12] Reactions were carried out under nitrogen, using distilled deionized water which was freshly de-carbonated prior to use by vigorously boiling for 15 minutes. As an example, a solution of $Zn(NO_3)_2{\cdot}6H_2O$ (2.97 g, 10 mmol) and $Al(NO_3)_3{\cdot}9H_2O$ (1.88 g, 5 mmol) in decarbonated water (20 mL) was added dropwise to a solution of 1,1′-ferrocenedicarboxylic acid (1.37 g, 5 mmol) and 50% NaOH (3.25 g, 40 mmol) in decarbonated water (35 mL) with efficient mixing. Once addition was complete, the resultant light brown gel-like slurry was stirred for 48 h at 75 °C. The solid was isolated by filtration, washed several times with de-carbonated water and dried at room temperature under reduced pressure in a vacuum desiccator. This material is referred to as $Zn_2Al-Fc(COO)_2$. The same general method was used for the synthesis of $Zn_2Al-FcCOO$ (10 mmol ferrocenecarboxylic acid). In both cases, the pH at the end of the reaction was in the range of 7−8.

$Zn_2Al-Fc(COO)_2$: $Zn_{3.8}Al_2(OH)_{11.6}[Fc(COO)_2]{\cdot}7H_2O$ (897.87): calcd. Zn 27.68, Al 6.01, Fe 6.22, C 16.05; found Zn 27.60, Al 6.04, Fe 6.22, C 15.29. TGA up to 180 °C revealed a sample weight loss of 13.1% (calcd: for loss of $7H_2O$, 14.0%; for loss of $6H_2O$, 12.3%). IR (KBr): $\tilde{\nu}$ = 3420 cm^{-1} (br), 2370 (w), 1554 (s), 1487 (m), 1460 (m), 1401 (m), 1389 (m), 1364 (m), 1347 (sh), 1260 (sh), 1193 (w), 1053 (sh), 1026 (m), 821 (m), 798 (m), 625 (m), 564 (m), 518 (m), 485 (w), 427 (s). Raman (cm^{-1}): 3362, 3117, 1480, 1459, 1392, 1367, 1195, 1070, 1034, 922, 569, 504, 324. ^{13}C CP MAS NMR: δ = 70.7 (*C*H), 79.5 (*C*−CO_2^-), 177.0 (C−*C*O_2^-). ^{27}Al MAS NMR: δ = 14.1 ppm.

$Zn_2Al-FcCOO$: $Zn_{3.5}Al_2(OH)_{11}[FcCOO]_2{\cdot}8H_2O$ (1072.1): calcd. Zn 21.34, Al 5.03, Fe 10.42, C 24.65; found Zn 21.40, Al 4.97, Fe 10.80, C 25.79. TGA up to 150 °C revealed a sample weight loss of 10.6% (calcd: for loss of $8H_2O$, 13.4%; for loss of $6H_2O$, 10.4%). IR (KBr): $\tilde{\nu}$ = 3407 cm^{-1} (br), 3086 (sh), 2924 (sh), 2861 (sh), 2367 (w), 2342 (w), 1525 (s), 1472 (m), 1391 (m), 1361 (m), 1347 (sh), 1266 (sh), 1211 (sh), 1187 (w), 1105 (w), 1024 (m), 1005 (w), 918 (w), 841 (sh), 819 (m), 793 (m), 637 (m), 554 (m), 510 (m), 485 (m), 429 (s). Raman (cm^{-1}): 3390, 3108, 1473, 1411, 1392, 1361, 1188, 1107, 1060, 1032, 918, 560, 504, 382, 314. ^{13}C CP MAS NMR: δ = 69.8 (*C*H), 77.8 (*C*−CO_2^-), 179.9 (C−*C*O_2^-). ^{27}Al MAS NMR: δ = 14.6 ppm.

Acknowledgments

The authors are grateful to FCT, POCTI and FEDER for financial support (Project POCTI//QUI/37990/2001). SG thanks the University of Aveiro for a research grant. Paula Esculcas and Claudia Morais are acknowledged for assistance with the NMR experiments.

[1] *Layered Double Hydroxides: Present and Future* (Ed.: V. Rives), Nova Science Publishers, Inc., New York, **2001**.
[2] A. I. Khan, D. O'Hare, *J. Mater. Chem.* **2002**, *12*, 3191−3198.
[3] [3a] S. P. Newman, W. Jones, *New J. Chem.* **1998**, 105−115. [3b] V. Rives, M. A. Ulibarri, *Coord. Chem. Rev.* **1999**, *181*, 61−120.
[4] B. F. Sels, D. E. De Vos, P. A. Jacobs, *Catal. Rev. −Sci. Eng.* **2001**, *43*, 443−488.
[5] P. Wang, G. Zhu, *Electrochem. Commun.* **2002**, *4*, 36−40.
[6] [6a] S. Morlat-Thérias, C. Mousty, P. Palvadeau, P. Molinié, P. Léone, J. Rouxel, C. Taviot-Guého, A. Ennaqui, A. de Roy, J. P. Besse, *J. Solid State Chem.* **1999**, *144*, 143−151. [6b] S. Therias, B. Lacroix, B. Schöllhorn, C. Mousty, P. Palvadeau, *J. Electroanal. Chem.* **1998**, *454*, 91−97.
[7] M. Ogawa, K. Kuroda, *Chem. Rev.* **1995**, *95*, 399−438.
[8] [8a] M. Vucelic, G. D. Moggridge, W. Jones, *J. Phys. Chem.* **1995**, *99*, 8328−8337. [8b] F. Kooli, I. C. Chisem, M. Vucelic, W. Jones, *Chem. Mater.* **1996**, *8*, 1969−1977. [8c] S. P. Newman, S. J. Williams, P. V. Coveney, W. Jones, *J. Phys. Chem. B* **1998**, *102*, 6710−6719.
[9] N. Iyi, K. Kurashima, T. Fujita, *Chem. Mater.* **2002**, *14*, 583−589.
[10] V. Prevot, C. Forano, J. P. Besse, F. Abraham, *Inorg. Chem.* **1998**, *37*, 4293−4301.
[11] G. Dong, L. Yu-ting, D. Chun-ying, M. Hong, M. Qing-jin, *Inorg. Chem.* **2003**, *42*, 2519−2530.
[12] M. A. Drezdon, *Inorg. Chem.* **1988**, *27*, 4628−4632.
[13] U. Costantino, N. Coletti, M. Nocchetti, G. G. Aloisi, F. Elisei, *Langmuir* **1999**, *15*, 4454−4460.
[14] [14a] W. Kagunya, R. Baddour-Hadjean, F. Kooli, W. Jones, *Chem. Phys.* **1998**, *236*, 225−234. [14b] J. T. Kloprogge, R. L. Frost in *Layered Double Hydroxides: Present and Future* (Ed.: V. Rives), Nova Science Publishers, Inc., New York, **2001**, pp. 139−192.
[15] F. Thevenot, R. Szymanski, P. Chaumette, *Clays Clay Miner.* **1989**, *37*, 396−402.
[16] J. Rocha, M. del Arco, V. Rives, M. A. Ulibarri, *J. Mater. Chem.* **1999**, *9*, 2499−2503.
[17] [17a] F. Kooli, C. Depège, A. Ennaqadi, A. De Roy, J. P. Besse, *Clays Clay Miner.* **1997**, *45*, 92−98. [17b] I. Crespo, C. Barriga, M. A. Ulibarri, G. González-Bandera, P. Malet, V. Rives, *Chem. Mater.* **2001**, *13*, 1518−1527. [17c] F. Rey, V. Fornés, *J. Chem. Soc., Faraday Trans.* **1992**, *88*, 2233−2238.
[18] A referee suggested that the observed collapse of the interlayer distance for $Zn_2Al-Fc(COO)_2$ upon heating could be due to the removal of water molecules present between the carboxylate groups and the positive charges. Based on the agreement between calculated and experimental interlayer spacings, we firmly believe that the collapse is due to a reorientation of guest species (analogous to that reported in the literature for LDHs pillared by terephthalate anions).
[19] L. Frydman, J. S. Harwood, *J. Am. Chem. Soc.* **1995**, *117*, 5367−5368.
[20] J. P. Amoureux, C. Fernandez, S. Steuernagel, *J. Magn. Reson., Sect. A.* **1996**, *123*, 116−118.

Received September 11, 2003
Early View Article
Published Online February 16, 2004

